

Low incidence rate of COVID-19 undermines confidence in estimation of the vaccine efficacy

Yasin Memari¹

1 MRC Cancer Unit, University of Cambridge, Cambridge CB2 0XZ, UK

Abstract

Knowing the true effect size of clinical interventions in randomised clinical trials is key to informing the public health policies. Vaccine efficacy is defined in terms of the ratio of two risks, however only approximate methods are available for the variance of the ‘risk ratio’. In this article, we show using a probabilistic model that uncertainty in the efficacy rate could be underestimated when the disease risk is low. Factoring in the baseline rate of the disease we estimate broader confidence intervals for the efficacy rates of the vaccines recently developed for COVID-19. We propose a new method for calculating the sample size in case-control studies where the efficacy is of interest. We further discuss the deleterious effects of classification bias which is particularly relevant at low disease prevalence.

Introduction

Vaccines are seen as the best control measure for the coronavirus pandemic. In this context, understanding the true efficacy of the vaccines and clinical interventions is crucial. Randomised clinical trials are conducted to systematically study the safety and the efficacy of an intervention in a subset of the population before it is widely used in the general population. In placebo-controlled vaccine trials, participants are randomised into vaccinated and unvaccinated groups where cases of the disease or infection are allowed to accrue over time. In planning a trial, advance sample size calculation determines the size of the trial population needed to detect a minimal clinically relevant treatment effect if such an effect exists. The indicator for effectiveness of a vaccine is usually reduction of the cases in the vaccinated group relative to the control group. However, it is sometimes naively assumed that the trial participants who do not experience the event provide no information. In consequence, the event rate or the incidence rate of the disease receives inadequate attention. For rare diseases, it is simply accepted that the accrual of the cases takes longer. Meanwhile, when an interim analysis declares a significant finding, the original assumptions used to define the power of the study and the sample sizes are often neglected. [1]

In this article our interest is on evaluating the impact of the event rate, insofar as it could affect the estimation of the efficacy rate. We show that low incidence rate of the disease could lead to overestimation of confidence in the estimated efficacy rates. We propose a new method for posterior of the efficacy rate which has a more subtle relationship with the event rate. Using our approach, we obtain broader confidence intervals for the efficacy of the vaccines recently developed for COVID-19. A new method for sample size calculation for vaccine efficacy trials is

proposed which is more robust at low incidence rates. Also highlighted is the impact of classification bias which could have large consequences when the disease risk is low.

Methods

Vaccine efficacy is defined as the proportionate reduction in the risk of disease or infection in a vaccinated group compared to an unvaccinated group. It is defined as $(1 - RR) \times 100\%$ in terms of the relative risk or risk ratio, $RR = \pi_v/\pi_c$, where π are the incidence of the disease among those exposed in the vaccinated and control groups. Throughout this paper we interchangeably use the terms, incidence rate, disease risk, prevalence and event rate. Assuming equal person-time exposure in the two groups, the *efficacy* is often summarised as

$$\alpha = 1 - \frac{\pi_v}{\pi_c} \simeq 1 - \frac{t_v}{t_c}, \quad (1)$$

where t_v and t_c are numbers of cases in the vaccinated and control groups.

It appears in the literature that only approximate methods are available for confidence intervals on the ‘risk ratio’ [2,3]. The consensus method which is quoted in numerous textbooks and papers is credited to Katz et al [3]. The method is based on asymptotic normality of logarithm of ratio of two binomial variables. Assuming independence of the incidence rates, it follows that $\text{var}(\log(\pi_v/\pi_c)) = \text{var}(\log(\pi_v)) + \text{var}(\log(\pi_c))$. Using a Taylor series, the variances are approximated as $\text{var}(\log(\pi)) \approx \text{var}(\pi)/\pi^2$ where Wald method is often used to set $\text{var}(\pi)$. Then two-sided 95% confidence intervals on the efficacy that are frequently used (e.g. see [4–7]) can be written as

$$95\%CL : 1 - \exp \left(\ln(RR) \pm 1.96 \sqrt{\frac{1 - \pi_v}{t_v} + \frac{1 - \pi_c}{t_c}} \right). \quad (2)$$

Hereafter we refer to equation 2 as pooled Wald approximation. We will argue that it underestimates the variance when the incidence rate is low. Firstly, Wald method is not appropriate when binomial probability is too small. One may use alternative binomial proportion confidence intervals, however, when π_v and π_c are small, log of their ratio might not be the difference of the logarithms or may be undefined [2]. Hightower et al [5] raised question about the credibility of the confidence limits when the efficacy is high and the disease risk is low. Also, as O’Neill noted [8], where $t \ll n$, the variance of $\ln(RR)$ in equation 2 remains fairly stable and quickly converges to $1/t_v + 1/t_c$. Independence of the probabilities of the incidence rates is also neither necessary nor ideal when calculating the efficacy as equation 1 imposes a constraint on the two variables.

To demonstrate the effect of the prevalence we model the vaccine efficacy in terms of conditional binomial probabilities. Under a binomial model with overall prevalence of π in both groups and total population size of n , overall number of cases $t = t_c + t_v$ follows $t \sim \text{Bin}(n, \pi)$, then assuming $t_c \sim \text{Bin}(t, 1/(2 - \alpha))$ we expect $t_c \sim \text{Bin}(n, \pi/(2 - \alpha))$. Were we to use Poisson distributions for t and t_c , t_c conditional on t would still follow a binomial distribution. The use of conditional distributions to model the efficacy has previously been suggested [4] and considerably simplifies the form of the likelihood function in terms of the incidence rate π .

For a general solution accounting for classification bias we assume an imperfect diagnostic procedure with sensitivity Se and specificity Sp . Then fraction of individuals who test positive for

the disease is sum of true positive rate and false positive rate:

$$\begin{aligned} T &= \text{Se} \times \pi + (1 - \text{Sp}) \times (1 - \pi) \\ &= c_1 + c_2\pi, \end{aligned} \quad (3)$$

where $c_1=1-\text{Sp}$ is the false positive rate and $c_2=\text{Se}+\text{Sp}-1$. The posterior distribution of α given that t_c is binomial follows as

$$\begin{aligned} p(\alpha|t_c, \pi, c_1, c_2) &= \frac{p(t_c|\alpha, \pi, c_1, c_2)p(\pi)p(\alpha)}{g(\alpha)} \\ &\propto \frac{1}{g(\alpha)} \binom{n}{t_c} \left(\frac{c_1 + c_2\pi}{2 - \alpha}\right)^{t_c} \left(1 - \frac{c_1 + c_2\pi}{2 - \alpha}\right)^{n-t_c} f(\pi), \end{aligned} \quad (4)$$

where $f(\pi)$ is the prior on π and we have assumed uniform prior on the efficacy $\alpha \sim \text{unif}\{0, 1\}$. For a complete solution, the marginal likelihood $g(\alpha)$ can be written in terms of the incomplete beta function (see e.g. [9]):

$$\begin{aligned} g(\alpha) &= f(\pi) \binom{n}{t_c} (c_1 + c_2\pi) \{B(c_1 + c_2\pi; t_c - 1, n - t_c + 1) \\ &\quad - B((c_1 + c_2\pi)/2; t_c - 1, n - t_c + 1)\}. \end{aligned}$$

As we do not intend to impose a prior on the prevalence, $f(\pi)$ in equation 4 cancels out and our analysis, in essence, is likelihood based. One needs to remember that, the posterior of equation 4, as it was derived from equation 1, is valid only when the individuals are equally divided between the two groups. The mode of the posterior of α is obtained by setting the derivative of the log likelihood to zero i.e. $\partial\ell/\partial\alpha = \partial\ln(p(\alpha|t_c, \pi))/\partial\alpha = 0$. This leads to

$$\alpha_{mode} = 2 - \frac{n(c_1 + c_2\pi)}{t_c}, \quad (5)$$

which corresponds to the maximum likelihood estimator (MLE). Cramér–Rao bound expresses a lower bound on the variance of any unbiased estimator of α in terms of the inverse of the Fisher information

$$\text{Var}(\alpha_{mode}) \geq \frac{1}{\mathcal{I}(\alpha)}, \quad (6)$$

where the Fisher information $\mathcal{I}(\alpha)$ is obtained as

$$\begin{aligned} \mathcal{I}(\alpha) &= \mathbb{E}\left[\left(\frac{\partial}{\partial\alpha}\ell(\alpha|t_c, \pi)\right)^2\right] = n \times \mathbb{E}\left[\left(-\frac{1-t_c}{2-\alpha-\pi} - \frac{-1}{2-\alpha}\right)^2\right] \\ &= \frac{n(c_1 + c_2\pi)}{(2-\alpha)^2(2-\alpha-(c_1 + c_2\pi))}. \end{aligned} \quad (7)$$

Here \mathbb{E} denotes ‘expected’ over t_c , where we have substituted $\mathbb{E}[t_c] = \mathbb{E}[t_c^2] = (c_1 + c_2\pi)/(2 - \alpha)$. We will show that the variance given by equation 6 has a more subtle dependence on π compared to equation 2. Under certain regularity conditions and assuming asymptotic normality near MLE, 95% confidence intervals on α_{mode} can be estimated as

$$\alpha_{mode} \pm \frac{1.96}{\sqrt{\mathcal{I}(\alpha_{mode})}}. \quad (8)$$

However, as the posterior distribution is asymmetric about the point estimator especially when the efficacy is high, in the next section we estimate the credible intervals computationally.

Results

Effect of incidence rate on vaccine efficacy

The posterior probability of vaccine efficacy given in its simplest form in equation 4 is now ready for our inspection. Using binomial notation is particularly useful in enabling us to directly plug in the numbers n , t_c in the estimation of α . In this section we evaluate the impact of the incidence rate on the efficacy and assign new confidence bounds to the efficacy of COVID-19 vaccines.

Firstly, we assume a diagnostic test with perfect sensitivity and specificity i.e. $Se=Sp=1$. In the absence of misclassification, mode of the posterior in equation 5 corresponds to the expectation $\hat{\alpha} = 1 - t_v/t_c$. The larger n the smaller the variance of the posterior, however, for a fixed n , the variance depends on π . Figure 1 shows the posterior probability of α plotted over a range of π , for a fixed n on the left hand, and for a fixed t on the right hand, assuming true vaccine efficacy of 70% and 90% respectively. Also plotted in vertical lines are the independent 95% confidence intervals from equation 2. As the event rate falls, the posterior distributions and the confidence intervals become wider, however, for a fixed t (right plot) Wald intervals are stable over a wide range of π , and more so when the efficacy is high. The proposed posterior probability better represents the variability at low prevalence.

Three clinical trials of the vaccines designed to prevent COVID-19 recently published their interim phase 3 analysis results [10–12] with two of them reporting incredibly narrow 95% confidence bounds on the efficacy. The reported case numbers and the efficacy rates for the primary end points are provided in Table 1. Firstly, we note that, although the trials used different models and priors on α , the reported confidence intervals almost perfectly correspond with those obtained from equation 2. At large n the posterior is clearly dominated by the data

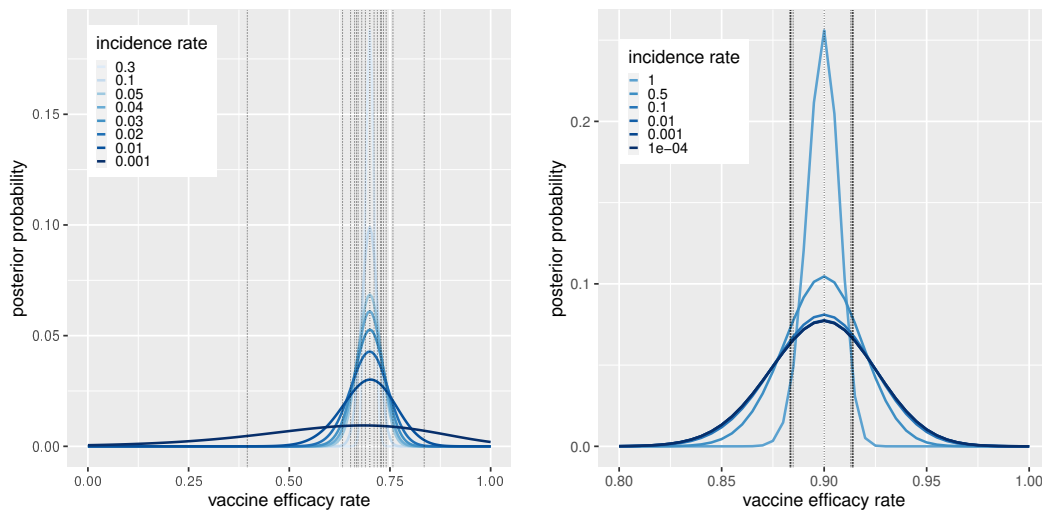


Figure 1. Posterior distribution of vaccine efficacy. Blue lines represent the posterior probability, while vertical lines show the independent Wald confidence intervals. Left hand plot assumes a fixed $n=50,000$ while right hand plot is for a fixed $t=2,000$. The general trend holds for different values of the parameters. Wald method overstates the confidence in α when $t \ll n$.

Table 1. Estimated efficacy of the vaccine trials

Trial	Case numbers and reported efficacy rates			Estimated efficacy rate
	case rate in vaccinated	case rate in control	reported efficacy and 95% CI	estimated mode and 95% credible interval
AZ-Oxford (combined)	30/5,807	101/5,829	70.4% [54.8, 80.6]	70.3% [39.1, 90.9]
Pfizer-BioNTech	8/18,198	162/18,325	95.0% [90.3, 97.6]	95.1% [74.9, 99.6]
Moderna-NIH	11/14,134	185/14,073	94.1% [89.3, 96.8]	94.1% [75.4, 99.5]

and the Bayesian and the frequentist are equivalent. Furthermore, especially where the efficacy is high, Wald confidence intervals hardly vary by the choice of n . If one were to use different values for n in Table 1, over a large range of the values equation 2 would still give the same confidence intervals. Therefore, the uncertainty caused by n_v and n_c is not accounted for.

We re-estimate the confidence intervals using the conditional binomial model presented in the Methods. Using the case numbers reported, the likelihood of the data in equation 4 is obtained by setting the prevalence to $\pi = T = t/n$. Then maximum *a posteriori* (MAP) and 95% credible intervals for the efficacy rates are calculated computationally. The results shown in Table 1 are contrasted with those reported. Although estimated modes are the same, our credible intervals are wider. Incorporating the incidence rates has removed the overwhelming weights originally assigned to confidence in estimation of the efficacy rates.

Note that, our approach requires the trial participants to be equally divided between the vaccinated and unvaccinated groups which is roughly the case here. Also of note is that, if we assume $\pi = t/n = 1$, the posterior in equation 4 produces the same intervals as those reported by the vaccine trials and Wald approximation.

Bias in case classification

So far we have assumed no bias in classification of the cases, however, imperfect diagnostic procedure could lead to misclassification of the infected and uninfected individuals. In this section we examine the effect of classification bias on estimation of the efficacy.

It is worth noting that equation 3 requires the observed infection rate T to be greater than the false positive rate $c_1 = 1 - Sp$. This relates to the ‘false positive paradox’ which implies that the accuracy of a diagnostic test is compromised if the test is used in a population where the incidence of the disease is lower than the false positive rate of the test itself. Furthermore, false negatives could dominate at low incidence rates. When the disease risk is low, as the majority of the tests are negative, a small false negative rate could lead to a situation where false negatives outnumber the positive cases. These concepts are further explained in Note 1.

Figure 2 illustrates the effect of classification bias on the posterior probability of the vaccine efficacy. The left plot shows the impact of a very small reduction in specificity to 0.999 (or increase in false positive rate), while the right hand plot shows the effect of reduction in sensitivity to 0.95 (or increase in false negative rate). A small loss of specificity could lead to serious underestimation of the effect size as noted by [6, 7], but it could further lead to complete loss of precision when the incidence rate is low. Loss of sensitivity results in overestimation of the efficacy irrespective of the disease rate. In these plots, we have considered a larger reduction in sensitivity, not only because reduction in specificity has a more dramatic effect, but also as

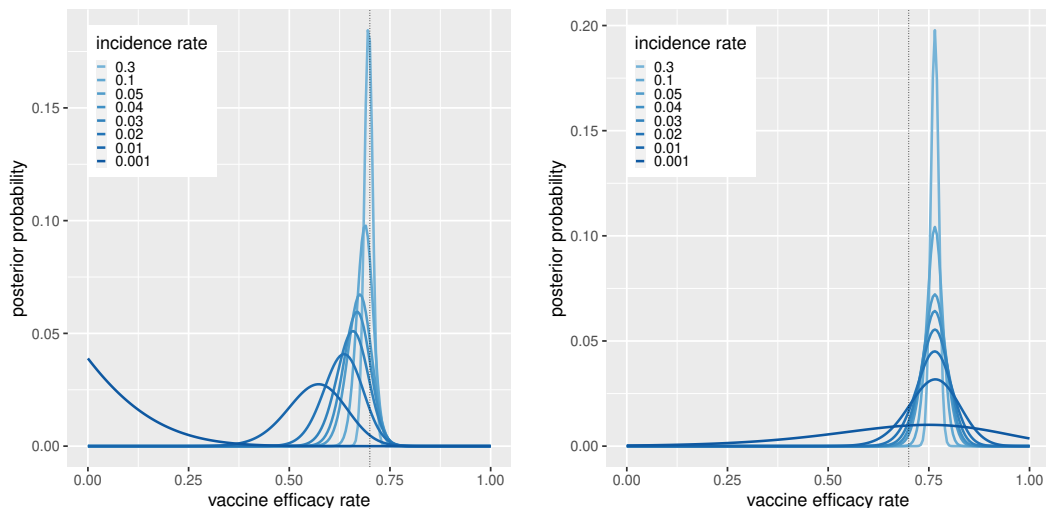


Figure 2. Effect of imperfect diagnostic procedure. Misclassification error biases the vaccine efficacy rate. Left plot shows the distributions for $Se=1$ and $Sp=0.999$, while the right plot is for $Se=0.95$ and $Sp=1$, with $n=50,000$ in both. True efficacy rate is assumed at 70%. Imperfect specificity, however small, could have disastrous effects when incidence rate is low, whereas lack of sensitivity consistently inflates the efficacy rate.

diagnostic assays typically have relatively higher specificity than sensitivity, not least due to specimen collection, insufficient viral load, stage of the disease, etc. [13] However, the effect of loss of sensitivity is consistently toward shifting the mode in equation 5, or MAP, to higher values of α , even at low incidence rates where negative predictive value is high.

Discussion

Base rate fallacy happens in situations where base rate information is ignored in favour of individuating evidence. In probability terms, it often occurs when $P(A|B)$ is confused or interchangeably used with $P(B|A)$ e.g. probability of having a rare disease given a positive test is wrongly equated to probability of a positive test given the disease (or diagnostic sensitivity) ignoring the low prior probability of the disease itself. We showed, in estimation of the vaccine efficacy, not only diagnostic error could have deleterious effects when the disease rate is low, but also failure to appropriately integrate the information about the base rate of the disease in the calculation could lead to underestimation of the uncertainty.

Vaccine efficacy is defined in terms of ratio of two risks, however only approximate methods are available for the variance of the ratio of two proportions. Ratio distributions are known to have heavy tails and usually no finite variance, while, conversely, Wald approximation may only serve as asymptotic variance of the risk ratio. We showed they result in grossly overoptimistic confidence bounds where the two proportions that are divided by each other are small. We proposed an alternative and simpler model for the efficacy that explicitly parametrises the likelihood in terms of π . Writing the likelihood function as $t_c \sim \text{Bin}(n, \pi/(2 - \alpha))$ is the natural choice as the probability of t_c is $\pi/(2 - \alpha)$. Instead of dividing the distributions for t_v and t_c , we

Note 1

J. Balayla [14] noted that there exists a *prevalence threshold* below which the positive predictive value (PPV) of a diagnostic test drops precipitously relative to the prevalence. This means that at too low a prevalence a positive test result could more likely be a false positive than a true positive. More underappreciated is the impact of the negative predictive value (NPV). Though, at low incidence rates, the negative predictive value is nearly 100%, a small loss in sensitivity could still have a marked effect as the negative tests vastly outnumber the positive tests. We could even have a situation where the false negatives are more than the true and false positives. To avoid these pitfalls, the participants are pre-selected for their symptoms before confirmation with the assay. Though this raises the pre-test probability, it could cause collider bias [15].

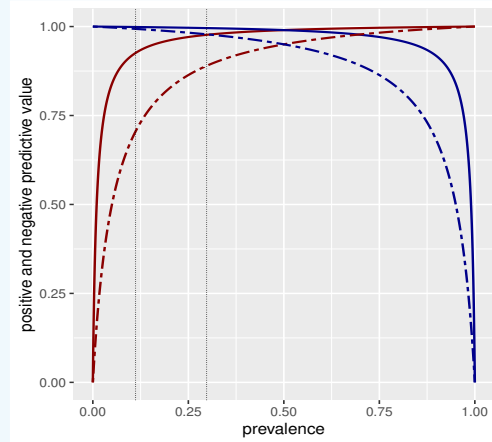


Figure 3. Positive (red) and negative (blue) predictive values are plotted in terms of population prevalence. Solid lines are for to a diagnostic test with $Se=Sp=0.99$; dashed lines are for $Se=Sp=0.95$. Vertical lines show the prevalence thresholds.

conditioned t_c on $t = t_c + t_v$ and treated t as another random variable $t \sim \text{Bin}(n, \pi)$. The resulting compound probability of t_c is over-dispersed and better captures the heterogeneity at low π . It serves to demonstrate the variability of the variance with π , whereas Wald approximation is largely insensitive to π when π is small. We solved the posterior without recourse to a prior distribution for π , however if one were to model the likelihood in terms of independent distributions, the choice of the prior would be critical. One has to remember that π_v and π_c are scaled binomials as they represent sample proportions. Uninformative priors could simply cancel out by the division and the dependence of the posterior on π would not become obvious.

Our findings have implications for pre-planning the sample sizes for phase 3 efficacy trials. Sample size calculation in case-control design is often stated as “How many samples are needed to be randomised in order to conclude with $100(1 - \beta)\%$ power that a treatment difference of size Δ exists between the two groups at the level of significance of α ?”. Therefore calculation of sample size requires specification of the null hypothesis (expected treatment effect) and the alternative hypothesis defined in terms of the difference in treatment outcomes. Here, α or type I error is the probability of rejecting the null hypothesis where we should not, and β or type II error is the probability of failing to reject the null hypothesis where we should reject it. Under the assumption of normality of the treatment outcome, a generic formula for per-group sample size is derived in terms of the two-sample t-test: [1]

$$n = \frac{2\sigma^2}{\Delta^2} (z_{1-\alpha/2} + z_{1-\beta})^2, \quad (9)$$

where z -scores determine the critical values for the standard normal distribution. Therefore one needs to specify the variance of the measured variable, the desired rates of error and the magnitude of the treatment difference. Where the measured variable is binary (infected or uninfected), the test statistic reduces to the test for the difference between two proportions. Where the efficacy is of interest, the log normal approximation of the risk ratio from equation 2 may be used to define the test statistic. O’Neill [8] calculated the required sample sizes for a two-sided test given the pooled Wald variance in equation 2. We re-write the *total* sample size in this form:

$$n = 2 \frac{(z_{1-\alpha/2} + z_{1-\beta})^2}{d^2} \left[\frac{(2 - \text{VE})^2}{\pi(1 - \text{VE})} - 2 \right], \quad (10)$$

where

$$d = \ln \left(\Delta / (2(1 - \text{VE})) + \sqrt{(\Delta / (2(1 - \text{VE})))^2 + 1} \right).$$

Here VE is the anticipated efficacy and Δ is the expected difference in VE in absolute terms. We showed, however, that at low prevalence rate, equation 2 significantly underestimates the variance. Using an inadequately small variance could lead to underestimation of the type I and type II errors, potentially resulting in winner’s curse in underpowered studies [16, 17]. If instead we were to use the proposed compound binomial model, one could simply substitute the variance in equation 6. As in [8], under the assumption of normality and assuming Δ is the difference between the upper and lower limits of the confidence interval, substituting the margin of error as $\Delta/2 = z\sigma$ in equation 6 gives

$$n \geq 4 \frac{(z_{1-\alpha/2} + z_{1-\beta})^2}{\pi \Delta^2} (2 - \text{VE})^2 (2 - \text{VE} - \pi). \quad (11)$$

This sets the *total* required sample size for a perfect diagnostic test, to be equally divided between the two groups.

The proposed Cramér–Rao bound based formula 11 assumes normality of distributions of the null and the alternative hypotheses, however, the binomial likelihood is asymmetric around its mode, as is Wald approximation (see [8]), and becomes more so as the efficacy increases and the prevalence decreases. Notwithstanding the limitations, we plug in the critical values for $\alpha = 0.05$ and power of $100(1 - \beta) = 80$ per cent ($z_{1-\alpha/2} = 1.96$ and $z_{1-\beta} = 0.84$) in equations 10 and 11. The resulting sample sizes are plotted in Figure 4 for $\Delta = 10\%$ and different prevalence and efficacy rates.

In Figure 4 the relationship between the sample size and the incidence rate looks linear on log-log scale as they have a power law relationship. However, while the two methods coincide at high incidence rates, Wald method significantly underestimates the sample sizes at low incidence rates especially when the efficacy is high (note that y-axis is on logarithmic scale). Contrasting Figure 4 with the case rates in Table 1, it is clear that, to achieve the narrow confidence bounds that Pfizer and Moderna have reported, they would have needed several times more samples under Wald method, and an order of magnitude more under Cramér–Rao bound. If the event rate were to differ from that in the general population or if possibility of misclassification was non negligible, such a discrepancy in incidence rates could cause such large variations in the variance that the trial population could be unrepresentative of the larger population. Table 2 provides the total sample sizes from Cramér–Rao bound formula 11 for different levels of efficacy and effect size. It is clear that the sample size is also very sensitive to the choice of Δ , therefore an investigator must be wary of misspecification of the anticipated treatment difference [1].

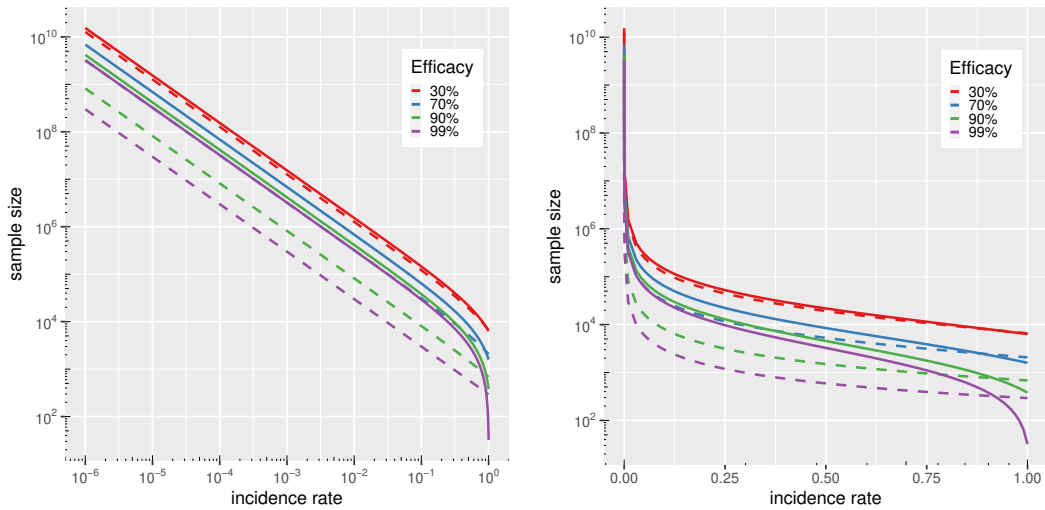


Figure 4. Sample size relative to disease prevalence. Total number of samples required to detect with 80% power and level of significance of $\alpha = 0.05$ a difference in the efficacy of size $\Delta = 10\%$. Solid lines represent Cramér–Rao bound and dashed lines represent Wald approximation. On the left, x-axis is on logarithmic scale. y-axis is logarithmic in both plots.

Table 2. Total sample sizes needed to conclude with 80% power and $\alpha=0.05$ a significant effect size

effect size		event rate						
VE	Δ	0.5	0.1	0.05	0.01	0.005	0.001	0.0005
0%	10%	37,632	238,336	489,216	2,496,256	5,005,056	25,075,456	50,163,456
0%	20%	9,408	59,584	122,304	624,064	1,251,264	6,268,864	12,540,864
0%	30%	4,181	26,482	54,357	277,362	556,117	2,786,162	5,573,717
0%	40%	2,352	14,896	30,576	156,016	312,816	1,567,216	3,135,216
30%	10%	21,751	145,009	299,080	1,531,654	3,072,371	15,398,105	30,805,273
30%	20%	5,438	36,252	74,770	382,913	768,093	3,849,526	7,701,318
30%	30%	2,417	16,112	33,231	170,184	341,375	1,710,901	3,422,808
30%	40%	1,359	9,063	18,693	95,728	192,023	962,382	1,925,330
60%	10%	11,064	79,905	165,957	854,372	1,714,890	8,599,037	17,204,221
60%	20%	2,766	19,976	41,489	213,593	428,723	2,149,759	4,301,055
60%	30%	1,229	8,878	18,440	94,930	190,543	955,449	1,911,580
60%	40%	691	4,994	10,372	53,398	107,181	537,440	1,075,264
90%	10%	4,553	37,946	79,686	413,607	831,009	4,170,221	8,344,237
90%	20%	1,138	9,486	19,921	103,402	207,752	1,042,555	2,086,059
90%	30%	506	4,216	8,854	45,956	92,334	463,358	927,137
90%	40%	285	2,372	4,980	25,850	51,938	260,639	521,515

Throughout the Methods section, we incorporated the misclassification error in the calculations in order to emphasise the importance of accounting for classification bias when the disease is rare. We showed that, while lack of diagnostic sensitivity consistently inflates the estimated efficacy rates, imperfect specificity results in serious loss of accuracy and precision at low disease risks. Case definition for COVID-19 is particularly a major caveat. The three vaccine trials broadly follow FDA definition of the disease. For primary end points symptomatic cases are identified by surveillance or are self-reported, and are subsequently confirmed with RT-PCR. Pre-selecting of the participants for PCR assay could create the possibility of collider bias [15]. Moreover, the highly non-specific symptoms of COVID-19, which include symptoms as common as cough and congestion, could create the perfect conditions for misclassification. False negatives due to e.g. selective reporting, specimen collection, etc, and PCR false positives due to e.g. remnant viral RNA, etc could be introduced if the test is not repeated [13, 18]. As much remains unknown about COVID-19 and its many symptoms and presentations, we recommend allowing for misclassification error in the calculation. The code for the posterior probability of the efficacy is provided. It can be used to simultaneously marginalise over the diagnostic sensitivity and specificity, as in [9].

Code

R code for posterior distribution of the efficacy (modified from code provided by [9]) along with functions to calculate the sample sizes from equations 10 and 11 are provided in the Appendix.

Acknowledgments

The author would like to appreciate the helpful comments from the Cancer Mutagenesis group at MRC Cancer Unit.

References

1. J. Wittes. Sample Size Calculations for Randomized Controlled Trials. *Epidemiologic Reviews*, 24(1):39–53, 07 2002.
2. J. J. Gart and J. Nam. Approximate interval estimation of the ratio of binomial parameters: a review and corrections for skewness. *Biometrics*, 44(2):323–338, Jun 1988.
3. D. Katz et al. Obtaining confidence intervals for the risk ratio in cohort studies. *Biometrics*, 34:469–474, 1978.
4. M. Ewell. Comparing methods for calculating confidence intervals for vaccine efficacy. *Stat Med*, 15(21-22):2379–2392, 1996.
5. A. W. Hightower et al. Recommendations for the use of Taylor series confidence intervals for estimates of vaccine efficacy. *Bull World Health Organ*, 66(1):99–105, 1988.
6. P. A. Lachenbruch. Sensitivity, specificity, and vaccine efficacy. *Controlled Clinical Trials*, 19(6):569 – 574, 1998.

7. A. Hahn et al. Impact of diagnostic methods on efficacy estimation – a proof-of-principle based on historical examples. *Tropical Medicine & International Health*, 25(3):357–363, 2020.
8. R. T. O’Neill. On sample sizes to estimate the protective efficacy of a vaccine. *Stat Med*, 7(12):1279–1288, Dec 1988.
9. P. J. Diggle. Estimating prevalence using an imperfect test. *Epidemiology Research International*, 2011(608719), 2011.
10. M. Voysey et al. Safety and efficacy of the ChAdOx1 nCoV-19 vaccine (AZD1222) against SARS-CoV-2: an interim analysis of four randomised controlled trials in Brazil, South Africa, and the UK. *Lancet*, Dec 2020.
11. F. P. Polack et al. Safety and efficacy of the bnt162b2 mrna covid-19 vaccine. *New England Journal of Medicine*, 383(27):2603–2615, 2020. PMID: 33301246.
12. L. R. Baden et al. Efficacy and safety of the mrna-1273 sars-cov-2 vaccine. *New England Journal of Medicine*, 0(0):null, 0.
13. I. Arevalo-Rodriguez et al. False-negative results of initial RT-PCR assays for COVID-19: A systematic review. *PLoS One*, 15(12):e0242958, 2020.
14. J. Balayla. Prevalence threshold and the geometry of screening curves. *PLoS One*, 15(10):e0240215, 2020.
15. G. J. Griffith et al. Collider bias undermines our understanding of COVID-19 disease risk and severity. *Nat Commun*, 11(1):5749, 11 2020.
16. J. P. Ioannidis. Why most discovered true associations are inflated. *Epidemiology*, 19(5):640–648, Sep 2008.
17. K. S. Button et al. Power failure: why small sample size undermines the reliability of neuroscience. *Nat Rev Neurosci*, 14(5):365–376, 05 2013.
18. J. Balayla. Bayesian updating and sequential testing: Overcoming inferential limitations of screening tests, 2020.

Appendix

```

#
# R function for Bayesian estimation of the efficacy rate using an
# imperfect test , originally modified from code provided by
# P. J. Diggle. Estimating prevalence using an imperfect test. \
# Epidemiology Research International , 2011(608719) , 2011
#
# Notes
#
# 1. Prior for efficacy rate is assumed uniform on (0,1)

```

```

# 2. Priors for sensitivity and specificity are independent scaled
# beta distributions
# 3. Function uses a simple quadrature algorithm with number of
# quadrature points as an optional argument "ngrid" (see below);
# the default value ngrid=20 has been sufficient for all examples
# tried by the author, but is not guaranteed to give accurate
# results for all possible values of the other arguments.
#
library(Rmpfr)
.N <- function(.) mpfr(., precBits = 200)

efficacy.bayes <- function(alpha, Tc, n, pi, lowse = 0.5, highse = 1.0,
                           sea = 1, seb = 1, lowsp = 0.5, highsp = 1.0,
                           spa = 1, spb = 1, ngrid = 20) {
  #
  # arguments
  # alpha: vector of efficacy rates for which posterior is required
  # (will be converted internally to increasing sequence of equally
  # spaced values, see "result" below)
  # Tc: number of positive test results
  # n: number of individuals tested
  # lowse: lower limit of prior for sensitivity
  # highse: upper limit of prior for sensitivity
  # sea, seb: parameters of scaled beta prior for sensitivity
  # lowsp: lower limit of prior for specificity
  # highsp: upper limit of prior for specificity
  # spa, spb: parameters of scaled beta prior for specificity
  # ngrid: number of grid-cells in each dimension for quadrature
  #
  # result is a list with components
  # alpha: vector of efficacy rate for which posterior density has
  # been calculated
  # post: vector of posterior densities
  # mode: posterior mode
  # interval: maximum a posteriori credible interval
  #
  ibeta <- function(x, a, b) {
    pbeta(x, a, b) * beta(.N(a), .N(b))
  }
  nalpha <- length(alpha)
  bin.width <- (alpha[nalpha] - alpha[1]) / (nalpha - 1)
  alpha <- alpha[1] + bin.width * (0:(nalpha - 1))
  integrand <- array(0, c(nalpha, ngrid, ngrid))
  h1 <- (highse - lowse) / ngrid
  h2 <- (highsp - lowsp) / ngrid
  for (i in 1:ngrid) {

```

```

se<-lowse+h1*(i-0.5)
pse<-(1/(highse-lowse))*dbeta((se-lowse)/(highse-lowse),sea,seb)
for (j in 1:ngrid) {
  sp<-lowsp+h2*(j-0.5)
  psp<-(1/(highsp-lowsp))*dbeta((sp-lowsp)/(highsp-lowsp),spa,spb)
  if (ngrid==1){
    se=highse; sp=highsp; pse=1; psp=1; h1=1; h2=1
  }
  c1<-1-sp
  c2<-se+sp-1
  g<-(c1+c2*pi)*chooseMpfr(n,Tc)*(ibeta(c1+c2*pi,Tc-1,n-Tc+1)-ibeta
    ((c1+c2*pi)/2,Tc-1,n-Tc+1))
  p<-(c1+c2*pi)/(2-alpha)
  density<-rep(0,nalpha)
  for (k in 1:nalpha) {
    density[k]<-asNumeric(dbinom(Tc,n,.N(p[k]))/g)
  }
  integrand[,i,j]<-pse*psp*density
}
}
post<-rep(0,nalpha)
for (i in 1:nalpha) {
  post[i]<-h1*h2*sum(integrand[i,,])
}

ord<-order(post,decreasing=Tc)
mode<-alpha[ord[1]]

cumpost=cumsum(post/sum(post))
interval=c(alpha[which.min(abs(cumpost-0.025))],
  alpha[which.min(abs(cumpost-0.975))])

list(alpha=alpha,post=post,mode=mode,interval=interval)
}
#
# example, to reproduce Table 1 results set ngrid=1, highse=1, highsp=1
# oxford 30 of 5807 vs 101 of 5829
# pfizer 8 of 18198 vs 162 of 18325
# moderna 11 of 14134 vs 185 of 14073

N<-14134+14073 # total number of participants
Tc<- 185 # number of cases in control
pi<- (185+11)/(14134+14073) # total number of cases / N

ngrid<-1
lowse<-1

```

```

highse<- 1 #0.95
lowsp<-1
highsp<-1 #0.999
sea<-2 #5
seb<-2
spa<-2 #5
spb<-2
alpha<-seq(0,1,by=0.0005) #0.001*(1:400)
result<-efficacy.bayes(alpha,Tc,N,pi,lowse,highse,
                        sea,seb,lowsp,highsp,spa,spb,ngrid)

result$mode
result$interval
plot(result$alpha,result$post/sum(result$post),type="l",xlab="alpha",
      ylab="p(alpha)")

# Function to reproduce per-group sample sizes presented in O'Neill,
# 1988. Note that he used relative width (RW) and attack rate in
# unvaccinated group (ARU)
sample_size_95wald_paper <- function(ARU,RW){
  VE=0.4
  y<-RW*VE/(2*(1-VE))
  d<-log(y+sqrt(y^2+1))
  return(((1.96)^2/d^2*((1+1/(1-VE))/ARU-2))
}
print(t(outer(c(0.01,0.005,0.001,0.0005),rev(seq(0.1,1,0.1))),
           sample_size_95wald_paper)),quote = FALSE)

# Total sample sizes for pooled Wald variance (power 80%
# and alpha=0.05)
sample_size_wald <- function(VE,Pi,delta){
  RW=delta/VE
  ARU=Pi/(2-VE)
  y<-RW*VE/(2*(1-VE))
  d<-log(y+sqrt(y^2+1))
  return(2*(1.96+0.84)^2/d^2*((1+1/(1-VE))/ARU-2))
}

# Total sample sizes for Cramer-Rao bound (power 80% and alpha=0.05)
sample_size_cramer <- function(VE,Pi,delta){
  return(4*(1.96+0.84)^2*(2-VE)^2*(2-VE-Pi)/Pi/delta^2)
}

```